Available online at www.sciencedirect.com
ScienceDirect
Journal of Nuclear Materials 376 (2008) 83–87
journal of nuclear materials
www.elsevier.com/locate/jnucmat

# Thermal properties of polycrystalline NdN bulk samples with various porosities

Jun Adachi *, Masahito Katayama, Ken Kurosaki, Masayoshi Uno, Shinsuke Yamanaka

*Division of Sustainable Energy and Environmental Engineering, Graduate School of Engineering, Osaka University, 2-1 Yamadaoka, Suita, Osaka 565-0871, Japan*

Received 13 November 2006; accepted 30 December 2007

**Abstract**

Neodymium mononitride (NdN) pellets with various porosities were prepared by a spark plasma sintering (SPS). The thermal expansion, specific heat capacity and thermal conductivity were measured and compared with those of uranium mononitride (UN), because NdN exists in the irradiated nitride fuels. The thermal expansion and specific heat capacity of NdN were very similar to those of UN. The thermal conductivity of the porosity-free NdN was estimated from the porosity dependence of the thermal conductivity. Unlike the case of the thermal conductivity of UN, that of NdN decreased with increasing temperature.


*PACS:* 65.40.−b (Thermal properties of crystalline solids); 65.40.Ba (Heat capacity); 65.40 (Thermal expansion, thermomechanical effects)

## 1. Introduction

The nitride fuel is a good candidate of the advanced fuels for FBR (Fast Breeder Reactor) [1,2] and ADS (Accelerator Driven System) [3,4] because of its superior properties, for example the high melting point, high metal density, high thermal conductivity, high chemical compatibility with the reactor core material and so on [1,2,5–8]. Therefore, the thermophysical properties of uranium mononitride (UN) [9–20], plutonium mononitride (PuN) [20–23] and uranium–plutonium mixed nitride ($U_XPu_{1-X}N$) [20,24–26] have been extensively studied. When we design the fuel assembly and evaluate the integrity of the nuclear fuel, it is very important to evaluate the thermophysical properties of the irradiated fuel. However, there are few data of the thermophysical properties of the irradiated nitride fuel because the research of the irradiated nitride fuel requires a lot of money and time. To evaluate the thermophysical properties of the high-burnup oxide fuels, SIMFUEL (SIMulated high-burnup FUEL) [27–33] is often used. Therefore, we are applying the concept of SIMFUEL to the nitride fuel, and evaluating the thermophysical properties of the simulated high-burnup nitride fuel. As a part of the research of the simulated high-burnup nitride fuel, we prepared the nitride fuel pellet containing neodymium nitride (NdN) and tried to evaluate the effect of NdN on the thermophysical properties of the nitride fuel. However, there are no data of the thermophysical properties of NdN because it is very difficult to prepare the bulk sample of NdN with high density and purity.

In the present study, we prepared the bulk samples of NdN with various densities by a SPS (Spark Plasma Sintering). The thermal expansion, specific heat capacity and thermal conductivity of NdN were evaluated and the results were compared with those of UN.

## 2. Experimental procedure

The crystal structure and lattice parameter of polycrystalline samples of NdN (Japan pure chemical Co. Ltd., 99.9%) were evaluated by the powder and bulk X-ray

* Corresponding author. Tel.: +81 6 6879 7905; fax: +81 6 6879 7889.
*E-mail address:* adachi@ms.see.eng.osaka-u.ac.jp (J. Adachi).

0022-3115/$ - see front matter © 2008 Elsevier B.V. All rights reserved.
doi:10.1016/j.jnucmat.2007.12.009

diffraction (XRD) methods using Cu Kα radiation at room temperature. The powder sample of NdN before the SPS was mixed with the epoxy resin and mounted on a folder for the XRD measurement in order to keep from oxidation. The bulk samples were prepared by the SPS (SPS Syntex Inc., Dr Sinter SPS-515S) at 1473, 1573, 1673 and 1773 K under a nitrogen atmosphere. The bulk samples prepared by the SPS were mounted on a folder for the XRD measurement. The bulk densities of the sintered samples were determined by the dimensions and weight. In order to determine the grain size before and after the SPS, the surface observations were performed by using a SEM (Scanning Electron Microscope) (HITACHI, S-2600H) and an optical microscope (OLYMPUS, BMX51M). From the SEM image of the powder sample, the maximum and minimum grain sizes were confirmed to be 40 μm and 20 μm, respectively. The grain size of the bulk sample was estimated from intervals of the grain boundaries crossing a straight line (300 μm) in the metallographic picture.

The thermal expansion ($\Delta L/L$) was measured by a thermodilatometry using BRUKER TD5020SA from 298 K to 873 K under nitrogen or an argon atmosphere with a flow rate of 100 ml/min. In the thermal expansion measurement, the heating rate was 5 or 10 K/min. As the standard sample, the column-shaped polycrystalline $Al_2O_3$ was used. The maximum deviation of the linear thermal expansion coefficient of $Al_2O_3$ measured in the present study from the TPRC (Thermal Property Research Center) data [34] was 3.2%. The results of $Al_2O_3$ were almost independent of the heating rate and atmosphere. In case of NdN, the heating rate, atmosphere and temperature rage were 5 K/min, nitrogen and from 298 K to 873 K, respectively.

The thermal conductivity ($\kappa$) was calculated using the following standard expression:

$$\kappa = D\frac{C_P}{M}\rho, \tag{1}$$

where $D$, $C_P$, $M$ and $\rho$ are the thermal diffusivity, specific heat capacity, molecular weight and density, respectively. $C_P$ was measured using a differential scanning calorimeter (DSC) (ULVAC, Triple-cell DSC) from 473 K to 1273 K under an argon atmosphere with flow rates of 50 or 100 ml/min. In the specific heat capacity measurement, the heating rate was 5 or 10 K/min. As the standard sample, the column-shaped sapphire was used. The maximum deviation of the specific heat capacity of sapphire measured in the present study from the SGTE (Scientific Group Thermodata Europe) data [35] was 6.2%. The results were almost independent of the heating rate and gas flow rate. In case of NdN, the heating rate and gas flow rate were 5 K/min and 100 ml/min, respectively. $D$ was measured by a laser flash method using ULVAC TC-7000 from 298 K to 1473 K in a vacuum ($10^{-4}$ Pa). Before we measure the thermal diffusivity, we waited until the temperature fluctuation was below 0.1 K/min. As the standard sample, the disk-shaped graphite was used. The maximum deviation of the thermal diffusivity of the graphite standard sample measured in the present study from the TPRC data [36] was 2.2%. $\rho$ was calculated from geometric measurements of the dimensions and weight and the thermal expansion data.

## 3. Results and discussion

From the XRD pattern of the powder sample, it was found that the single phase of NdN with NaCl type cubic structure was obtained in the present study. The SPS was performed for the powder sample. As the results of the SPS, six kinds of bulk samples of NdN were prepared. The sintering condition and density of each sample are summarized in Table 1. From the XRD patterns of the bulk samples, only the peaks corresponding to those of NdN could be observed. In addition, the lattice parameter calculated from the XRD pattern of the powder sample (=0.5124 nm) was very close to that of the bulk sample (=0.5127 nm). From these results, it was confirmed that the oxidation in the SPS process is vanishingly small. The lattice parameter of NdN (=0.5124 nm) was larger than that of UN (=4889 nm [9]). From the SEM and optical microscope observations, the grain size of the powder sample almost corresponded to those of the bulk samples. In addition, it was found that the pores were concentrated at the grain boundaries. The grain size of each sample is summarized in Table 1.

The thermal expansion behavior of NdN is shown in Fig. 1, together with the literature data of UN [9,14–16]. In addition, Fig. 2 shows the temperature dependence of the linear thermal expansion coefficient (LTEC) of NdN, together with the literature data of UN [9,13–17]. The density of the sample used in the thermodilatometry measurement was 89.2% of the theoretical density (%T.D.) (=7.879 g/cm$^3$), which was calculated from the crystal structure and lattice parameter obtained from the XRD analysis. The thermodilatometry measurements were per-

Table 1
Characteristics of NdN samples

| | | | | | | | |
|---|---|---|---|---|---|---|---|
| Sintering temperature | (K) | 1473 | 1573 | 1673 | 1773 | 1673 | 1773 |
| Heating rate of SPS[a] | (K/min) | 100 | 100 | 100 | 100 | 50 | 50 |
| Density | (g/cm$^3$) | 5.224 | 6.047 | 6.938 | 7.028 | 6.304 | 6.942 |
| Relative density | (%T.D.) | 66.3 | 76.8 | 88.1 | 89.2 | 80.1 | 88.2 |
| Grain size | (μm) | 20–40 | | | | | |

[a] SPS: Spark plasma sintering.

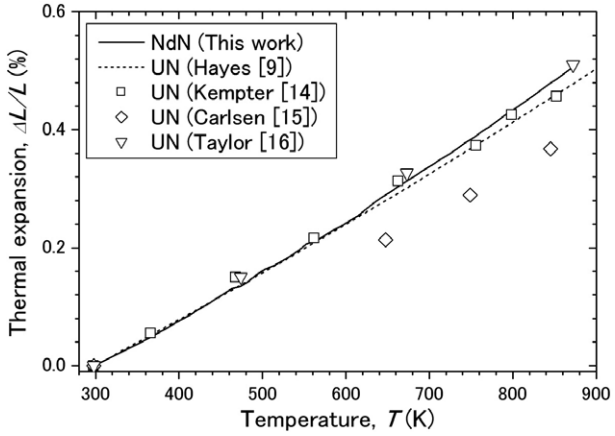


Fig. 1. Thermal expansion data of NdN, together with the literature data of UN [9,14–16].

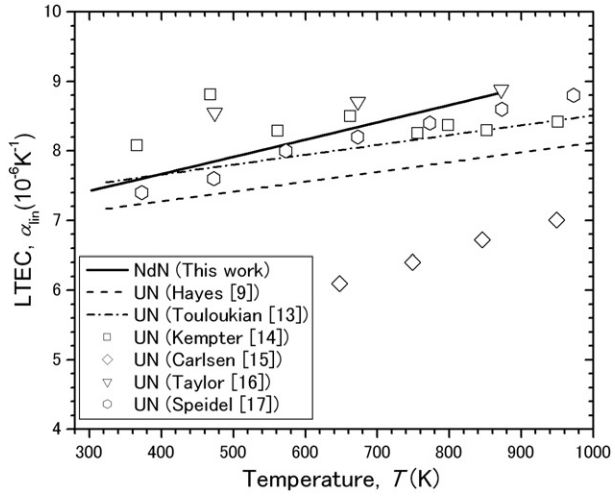


Fig. 2. Temperature dependence of the LTEC of NdN, together with the literature data of UN [9,13–17].

formed for three samples under the same conditions. The length ($X, Y, Z$) of the three rectangular-shaped samples are (6.26 mm, 3.28 mm, 2.68 mm), (6.89 mm, 6.13 mm, 2.51 mm) and (6.98 mm, 4.72 mm, 1.85 mm) and the thermal expansion in the $X$-dimension was measured. The thermal expansion behaviors of the three samples are consistent with each other. The thermal expansion of NdN can be expressed as the following equation:

$$\frac{\Delta L}{L}(\%) = \frac{L_T - L_{298}}{L_{298}}(\%) = 7.297 \times 10^{-4} \times (T - 298.15) + 2.665 \times 10^{-8} \times (T - 298.15)^2 \quad (298\ \mathrm{K} < T < 878\ \mathrm{K}), \tag{2}$$

where $T$ and $L_T$ are the absolute temperature and length of the sample at $T$ (K), respectively. From Fig. 2, the LTEC of NdN was very similar to that of UN. From these results, it is predicted that the thermal expansion of (U, Nd)N is similar to those of UN and NdN.

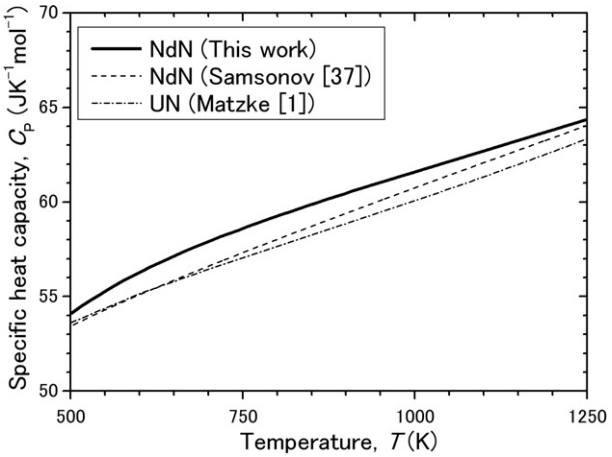


Fig. 3. Temperature dependence of the specific heat capacity of NdN, together with the literature data of NdN [37] and UN [1].

The temperature dependence of $C_P$ of NdN is shown in Fig. 3, together with the literature data of NdN [37] and UN [1]. The DSC measurements were performed for two samples under the same condition. The length ($X, Y, Z$) of the two rectangular-shaped samples used in the DSC measurements are (3.05 mm, 3.14 mm, 2.88 mm) and (2.89 mm, 3.03 mm, 2.91 mm). The $C_P$ of the two samples are consistent with each other. From the reproducibility in the results of the thermodilatometry and DSC measurements, it was confirmed that the data of NdN obtained in the present study were reliable. From Fig. 3, the $C_P$ of NdN obtained in the present study corresponded to the literature data [37] and was very similar to that of UN [1]. In the temperature range between 473 and 1273 K, the empirical equation for the $C_P$ of NdN was determined from the experimental data as follows:

$$C_P(\mathrm{JK^{-1}mol^{-1}}) = 53.33 + 9.245 \times 10^{-3} T - 9.488 \times 10^{5} T^{-2} \quad (473\ \mathrm{K} < T < 1273\ \mathrm{K}). \tag{3}$$

The thermal diffusivity was measured by the laser flash method for five bulk samples whose densities are 66.3, 76.8, 80.1, 88.1 and 88.2%T.D. The dimensions of the column-shaped samples with 66.3, 76.8, 80.1, 88.1 and 88.2%T.D. are φ10.37mm × h1.94 mm, φ10.53 mm × h1.75 mm, φ10.54 mm × h1.99 mm, φ9.36 mm × h1.60 mm and φ10.41 mm × h1.79 mm, respectively. By using the thermal expansion data (Eq. (2)), specific heat capacity data (Eq. (3)) and thermal diffusivity data, the thermal conductivity of each bulk sample of NdN was calculated. The temperature dependences of the thermal conductivity are shown in Fig. 4, together with the literature data of UN [11,19,20]. Fig. 5 shows the porosity ($P$) dependence of the relative thermal conductivity of NdN, together with the literature data of UN [19] and ZrN [39]. As shown in Fig. 4, the thermal conductivity of NdN on the heating process corresponds to that on the cooling process, which indicates that the effect of the oxidation during the laser flash measurements is vanishingly small. In Fig. 5, the

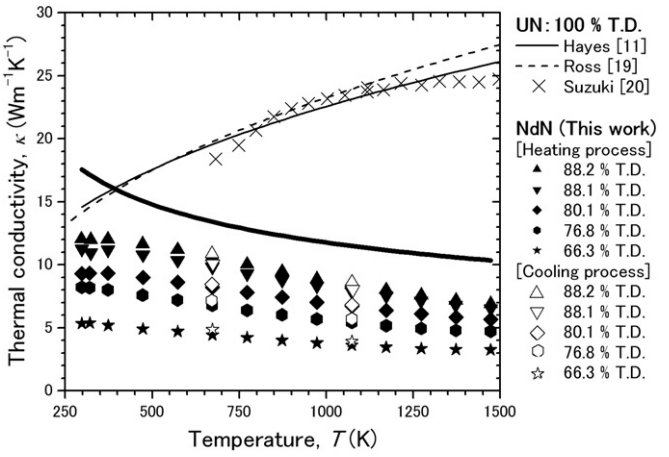


Fig. 4. Temperature dependence of the thermal conductivity of NdN, together with the literature data of UN [11,19,20]. The bold solid line represents the thermal conductivity of the porosity-free material of NdN estimated using the Maxwell–Eucken's equation.

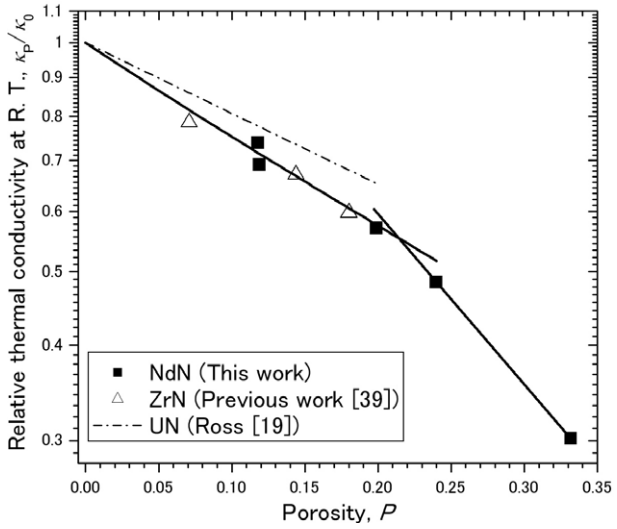


Fig. 5. Porosity dependence of the relative thermal conductivity of NdN at room temperature, together with the literature data of UN [19] and ZrN [39].

thermal conductivity exponentially decreased with increasing the porosity in the region of $P < 0.2$. On the other hand, the thermal conductivity rapidly decreased with increasing the porosity in the region of $P > 0.2$. From these results, it was found that the $P_C$ value existed between $P = 0.199$ (80.1%T.D.) and $P = 0.232$ (76.8%T.D.). The $P_C$ value represents the starting point of the rapid decrease of the thermal conductivity because the MSA (Minimum Solid Area) [38] rapidly decrease with increasing the porosity from the $P_C$ value. In Fig. 5, the bold solid line represents the fitting results for porosity dependence of the thermal conductivity in the region of $P < 0.2$ using the Maxwell Eucken's equation. From the fitting line, the porosity dependence of the thermal conductivity of NdN can be represented as the following equation:

$$\kappa(P) = \kappa(0)\frac{1-P}{1+\beta P}, \tag{4}$$

where $\beta$ is the correction factor and its value is 1.96. The thermal conductivity ($\kappa$) of the porosity-free material of NdN at each temperature was estimated and the temperature and porosity dependences of the thermal conductivity of NdN was revealed by the following equation:

$$\kappa(P,T) = 115T^{-0.330}\frac{1-P}{1+1.96P} \quad (298\ \mathrm{K} < T < 1473\ \mathrm{K},\ 0 < P < 0.2). \tag{5}$$

In our previous study [39], the $\beta$ for zirconium mononitride (ZrN) prepared by the SPS was 2.1, which is similar to that of NdN. This result is reasonable since it is well known that the $\beta$ indicates the similar value when the preparation method, grain size and pore shape of the bulk samples are the same in case of the same crystal structure [38]. In Fig. 4, the bold solid line represents the thermal conductivity of the porosity-free NdN (Eq. (5)). The thermal conductivity of UN increased with increasing temperature because the electronic contribution to the thermal conductivity is predominant [11]. On the other hand, that of NdN decreased with increasing the temperature. In addition, the thermal conductivity of NdN was lower than that of UN in the region of $T > 400$ K. Therefore, it was supposed that the thermal conductivity of (U, Nd)N decreases with increasing NdN content at the reactor core temperature.

## 4. Summary

Six bulk samples of NdN were prepared by the SPS and the thermal properties were evaluated. The XRD analysis and surface observation revealed that the lattice parameter and grain size of the samples before and after the SPS were very similar.

The thermal expansion of NdN was represented as the following equation:

$$\frac{\Delta L}{L}(\%) = \frac{L_T - L_{298}}{L_{298}}(\%) = 7.297\times10^{-4}\times(T-298) + 2.665\times10^{-8}\times(T-298)^2 \quad (298\ \mathrm{K} < T < 878\ \mathrm{K}).$$

The specific heat capacity of NdN was represented as the following equation:

$$C_P(\mathrm{JK^{-1}mol^{-1}}) = 53.33 + 9.245\times10^{-3}T - 9.488\times10^{5}T^{-2} \quad (473\ \mathrm{K} < T < 1273\ \mathrm{K}).$$

The thermal expansion and specific heat capacity of NdN were very similar to those of UN.

We estimated the temperature and porosity dependences of the thermal conductivity of NdN as the following equation:

$$\kappa(P,T) = 115T^{-0.330}\frac{1-P}{1+1.96P}$$
$$(298\ \mathrm{K} < T < 1473\ \mathrm{K},\ 0 < P < 0.2).$$

Unlike the thermal conductivity of UN, that of NdN decreased with increasing temperature indicating that the phonon contribution is predominant. The results obtained in the present study are very useful and important in evaluating the thermal properties of the irradiated nitride fuel.

## References


[1] H. Matzke, Science of Advanced LMFBR Fuels: Solid State Physics, Chemistry, and Technology of Carbides, Nitrides, and Carbonitrides of Uranium and Plutonium, Elsevier Science Publishing Co., Amsterdam, North-Holland, 1986.

[2] D. Brucklacher, W. Dienst, T. Dippel, O. Goetzmann, P. Hofmann, H. Holleck, H. Kleykamp, W. Siebmanns, F. Thuemmler, Neue. Technik. 13 (1971) 299.

[3] T. Sasa, H. Oigawa, K. Tsujimoto, K. Nishihara, K. Kikuchi, Y. Kurata, S. Saito, M. Futakawa, M. Umeno, N. Ouchi, Y. Arai, K. Minato, H. Takano, Nucl. Eng. Des. 230 (2004) 209.

[4] W. Gudowski, V. Arzhanov, C. Broeders, I. Broeders, J. Cetnar, R. Cummings, M. Ericsson, B. Fogelberg, C. Gaudard, A. Konning, P. Landeyro, J. Magill, I. Pazsit, P. Peerani, P. Philippen, M. Pintek, E. Ramstrom, P. Ravetto, G. Ritter, Y. Shubin, S. Soubiale, C. Toccoli, M. Valade, J. Wallenius, G. Youinou, Prog. Nucl. Energy 38 (2001) 135.

[5] J. Wallenius, J. Nucl. Mater. 320 (2003) 142.

[6] A.A. Bauer, P. Cybulskis, J.L. Green, Mixed-nitride fuel performance, in: EBR-II, Adv. LMFBR Fuels Top. Meet. Proc., Am. Nucl. Sci., 1977, p. 299.

[7] D. Brucklacher, Fak. Maschinenbau, Fed. Rep. Ger. Avail. INIS. Report, INIS-mf-5402 (1978) 101.

[8] A.K. Sengupta, C. Ganguly, Trans. Indian. Inst. Metal 43 (1990) 31.

[9] S.L. Hayes, J.K. Thomas, K.L. Peddicord, J. Nucl. Mater. 171 (1990) 262.

[10] S.L. Hayes, J.K. Thomas, K.L. Peddicord, J. Nucl. Mater. 171 (1990) 271.

[11] S.L. Hayes, J.K. Thomas, K.L. Peddicord, J. Nucl. Mater. 171 (1990) 300.

[12] S.L. Hayes, J.K. Thomas, K.L. Peddicord, J. Nucl. Mater. 171 (1990) 289.

[13] Y.S. Touloukian, R.K. Kirby, R.R. Taylor, T.Y.R. LeeThermophysical Properties of Matter, Thermal Expansion: Non-metallic Solids, vol. 13, IFI/Plenum, New York, Washington, 1977.

[14] C.P. Kempter, R.O. Elliott, J. Chem. Phys. 30 (1959) 1524.

[15] F.L. Carlsen, W.O. Harms, US At. Energy Comm. ORNL-3670 (1964) 56.

[16] K.M. Taylor, C.H. CmMurty, US At. Energy Comm. ORO-248 (1959) 21.

[17] E.O. Speidel, D.L. Keller, US At. Energy Comm. BMI-1633 (1963) 66.

[18] R. Benz, G. Balog, B.H. Baca, High Temp. Sci. 15 (1970) 221.

[19] S.B. Ross, M.S. El-Genk, R.B. Matthews, J. Nucl. Mater. 151 (1988) 313.

[20] Y. Suzuki, Y. Arai, J. Alloys Comp. 271–273 (1998) 577.

[21] D.F. Carroll, US At. Energy Comm. HW-75125 (1962) 10.

[22] C.A. Alexander, R.B. Clark, O.L. Krugar, J.L. Robins, Plutonium and other actinides 1975, in: Proc. Int. Conf. 5th, 1976, p. 277.

[23] F.L. Oetting, J. Chem. Thermodyn. 10 (1978) 941.

[24] C. Ganguly, P.V. Hedge, A.K. Sengupta, J. Nucl. Mater. 178 (1991) 234.

[25] Y. Suzuki, Y. Arai, T. Iwai, T. Ohmichi, J. Nucl. Sci. Technol. 28 (1991) 689.

[26] V.J. Tennery, E.S. Bomar, J. Am. Ceram. Soc. 54 (1971) 247.

[27] R.A. Verrall, I.J. Hastings, P.G. Lucuta, H. Matzke, B.J.F. Palmer, in: Annual Conference Proceedings – Canadian Nuclear Society 11th, 1990, p. 6.1.

[28] P.G. Lucuta, R.A. Verrall, H. Matzke, B.J. Palmer, J. Nucl. Mater. 178 (1991) 48.

[29] P.G. Lucuta, H. Matzke, R.A. Verrall, H.A. Tasman, J. Nucl. Mater. 188 (1992) 198.

[30] P.G. Lucuta, R.A. Verrall, H. Matzke, J. Hastings, in: Conf. Proc. – Int. Conf. CANDU Fuel Perform. 3rd, 1992, p. 2-61.

[31] P.G. Lucuta, H. Matzke, R.A. Verrall, J. Nucl. Mater. 217 (1994) 279.

[32] P.G. Lucuta, H. Matzke, R.A. Verrall, P.G. Klemens, Thermal conductivity, in: Proceedings of the 'International Thermal Conductivity Conference' and 'International Thermal Expansion Symposium', vol. 22, 1994, p. 894.

[33] H. Matzke, P.G. Lucuta, R.A. Verrall, J.P. Hiernaut, Thermal conductivity, in: Proceedings of the 'International Thermal Conductivity Conference' and 'International Thermal Expansion Symposium', vol. 22, 1994, p. 904.

[34] Y.S. Touloukian, R.K. Kirby, R.E. Taylor, T.Y.R. Lee, Thermal Expansion: Non-metallic Solid, IFI/Plenum, New York, 1977.

[35] The SGTE Pure Substance and Solution databases, GTT-DATA SERVICES, 1996.

[36] Y.S. Touloukian, R.W. Powell, C.Y. Ho, P.G. Klemens, Thermal Conductivity: Non-metallic Solid, IFI/Plenum, New York, 1970.

[37] G.V. Samsonov, I.M. Vinitskii, Handbook of Refractory Compounds, IFI/Plenum, New York, 1980.

[38] R.W. Rice, Porosity of Ceramics, Marcel Dekker Inc., New York, 1999.

[39] J. Adachi, K. Kurosaki, M. Uno, S. Yamanaka, J. Alloys Compd. 432 (2007) 7.